



Technical Report HCSU-101

## 2019–2021 PALILA ABUNDANCE ESTIMATES AND TREND

Ayesha S. Genz<sup>1</sup>, Kevin W. Brinck<sup>1</sup>, Chauncey K. Asing<sup>2</sup>, Lainie Berry<sup>3</sup>,  
Richard J. Camp<sup>4</sup>, and Paul C. Banko<sup>4</sup>

<sup>1</sup> Hawai'i Cooperative Studies Unit, University of Hawai'i at Hilo, 200 West Kawili St, Hilo, HI 96720

<sup>2</sup> University of Hawai'i at Mānoa, Pacific Cooperative Studies Unit, 3190 Maile Way, St John 408,  
Honolulu, HI 96822

<sup>3</sup> State of Hawaii, Department of Land and Natural Resources Division of Forestry and Wildlife,  
1151 Punchbowl St, Rm 325, Honolulu, HI 96813

<sup>4</sup> U.S. Geological Survey, Pacific Island Ecosystems Research Center, P.O. Box 44,  
Hawai'i National Park, HI 96718

University of Hawai'i at Hilo  
200 W. Kawili St.  
Hilo, HI 96720  
(808) 933-0706

January 2022



UNIVERSITY  
of HAWAII®  
**HILO**

Citation: Genz, A. S., K. W. Brinck, C. K. Asing, L. Berry, R. J. Camp, and P. C. Banko. 2022. 2019–2021 Palila abundance estimates and trend. Hawai'i Cooperative Studies Unit Technical Report HCSU-101. University of Hawai'i at Hilo, Hawaii, USA. 20 pp.

This product was prepared under Cooperative Agreement 21ZBCOLL05DOFRC for the U.S. Geological Survey Pacific Island Ecosystems Research Center.

*This article has been peer reviewed and approved for publication consistent with U.S. Geological Survey Fundamental Science Practices (<http://pubs.usgs.gov/circ/1367/>). Any use of trade, firm, or product names is for descriptive purposes only and does not imply endorsement by the U.S. Government.*

## TABLE OF CONTENTS

List of Tables .....	iii
List of Figures .....	iii
Abstract.....	1
Introduction.....	1
Methods .....	2
Bird Sampling .....	2
Abundance Estimation.....	4
Trend Detection.....	5
Sampling Condition Evaluation.....	6
Results .....	6
Abundance Estimation.....	6
Trend Detection.....	7
Sampling Condition Evaluation.....	13
Conclusions .....	13
Acknowledgements .....	14
Literature Cited .....	15

## LIST OF TABLES

Table 1. Number of transects and stations sampled by year inside and outside the core survey area .....	3
Table 2. Results of fitting 17 detection function models to the 1998–2021 palila distance histogram .....	8
Table 3. Annual palila detections and population estimate parameters.....	10

## LIST OF FIGURES

Figure 1. Palila survey area for the 2019–2021 surveys .....	2
Figure 2. Five blocks of years grouped by the similarity of the parameter coefficients.....	5
Figure 3. Palila detected per visit across 2019–2021 surveys.....	7
Figure 4. Hazard-rate detection function and probability density of the best-fit detection model.....	9
Figure 5. Annual palila population estimates from 1998 through 2021 .....	11
Figure 6. State-space model estimates of palila abundance over multiple time spans.....	12
Figure 7. Violin plots of weather covariates for each survey year .....	13

## ABSTRACT

The palila (*Loxioides bailleui*) population on Mauna Kea Volcano, Hawai'i Island, was estimated from annual surveys in 2019–2021, and a trend analysis was performed on survey data from 1998–2021. The 2019 population was estimated at 1,030–1,899 birds (point estimate: 1,432), the 2020 population was estimated at 964–1,700 birds (point estimate: 1,312), and the 2021 population was estimated at 452–940 birds (point estimate: 678). Since 1998, a visual inspection of the size of the area containing palila detections on the western slope based on the minimum/maximum elevations has not shown a substantial change, indicating that the range of the species has remained stable; although this area represents only about 5% of its historical extent. During 1998–2005, palila numbers fluctuated between 4,000 and 6,000, followed by a steep decline. After 2010, palila estimates stabilized around an abundance of 2,000 with a much slower rate of decline. The decline during 1998–2021 was on average 229 birds per year with very strong statistical support for an overall downward trend in abundance. Over the 23-year monitoring period, the estimated rate of change equated to an 89% decline in the population.

## INTRODUCTION

The palila (*Loxioides bailleui*) is an endangered, seed-eating, finch-billed Hawaiian honeycreeper (a distinct group within family Fringillidae: subfamily Drepanidinae) found only on Hawai'i Island. Once occurring on the islands of Kaua'i and O'ahu, as well as Mauna Loa and Hualālai volcanoes of Hawai'i, palila are now found only in subalpine, dry-forest habitats on the southwestern slope of Mauna Kea (Banko *et al.* 2002a). Previous analyses showed that palila numbers fluctuated throughout the 1980s and 1990s, but since 1998 palila have declined and they appear to have declined steadily since at least 2005 (Jacobi *et al.* 1996, Leonard *et al.* 2008, Banko *et al.* 2009, Gorresen *et al.* 2009, Banko *et al.* 2013, Genz *et al.* 2018).

Palila move up and down the western slope of Mauna Kea seasonally as they track the availability of seeds of the endemic māmane (*Sophora chrysophylla*) tree—their main food (Hess *et al.* 2001). During the time of the annual palila population surveys, which are usually performed in January to February, māmane seedpods are most abundant at higher elevations, but seedpod abundance increases at lower elevations by May (Banko *et al.* 2002b). Although the distribution of palila shifts in response to food availability, the areas that are occupied seasonally overlap extensively, and the area that is surveyed each winter provides a stable and representative basis for evaluating population abundance and trends.

This report updates abundance estimates and population trends for palila since 1998, incorporating new detection data from the 2019, 2020, and 2021 surveys. Although palila surveys have been conducted since 1980, additional transects were added to the original Hawaii Forest Bird Survey (HFBS, [https://bison.usgs.gov/ipt/resource?r=usgs\\_pierc\\_hfbs1](https://bison.usgs.gov/ipt/resource?r=usgs_pierc_hfbs1)) transects in 1998 to produce a more precise population estimate and provide more complete coverage of the palila distribution during the survey period (Johnson *et al.* 2006). As a result, our estimates are restricted to the period covering the modern survey effort (1998 through 2021).

## METHODS

### Bird Sampling

Since 1980, 95% of the palila population inhabited a 64.4 km<sup>2</sup> area on the southwestern slope of Mauna Kea (Scott *et al.* 1984, Banko *et al.* 2013, Camp *et al.* 2014; Figure 1). We refer to this area hereafter as the “core survey area.” During 5–7 February 2019, 4–26 February 2020, and 1–7 February 2021, point-transect sampling was conducted on Mauna Kea to estimate palila abundance and range. For all three years, 13 bird survey transects inside the core survey area (transects 101–108 and 122–126; Figure 1) were surveyed one or more times. In addition to the core survey area, supplemental transects to the east of the core range were surveyed in all three years to look for possible range expansion. These included transects 109 and 110 in 2019 and 2021, and transect 109 in 2020. Within the Ka’ohe mitigation area (Banko *et al.* 2009; Figure 1), surveys were conducted on supplemental stations in the lower portions of transects 101, 102, 124, and 125 in 2019; the lower portion of transect 125 in 2020; and the lower portions of 102, 124, and 125 in 2021. Within the core survey area, the 2019 survey consisted of 420 counts at 417 stations, the 2020 survey consisted of 421 counts at 419 stations, and the 2021 survey consisted of 422 counts at 420 stations (Figure 1, Table 1). The adjacent, supplemental stations outside of the core survey area were counted once in 2019 (83 counts), 2020 (23 counts), and 2021 (74 counts).

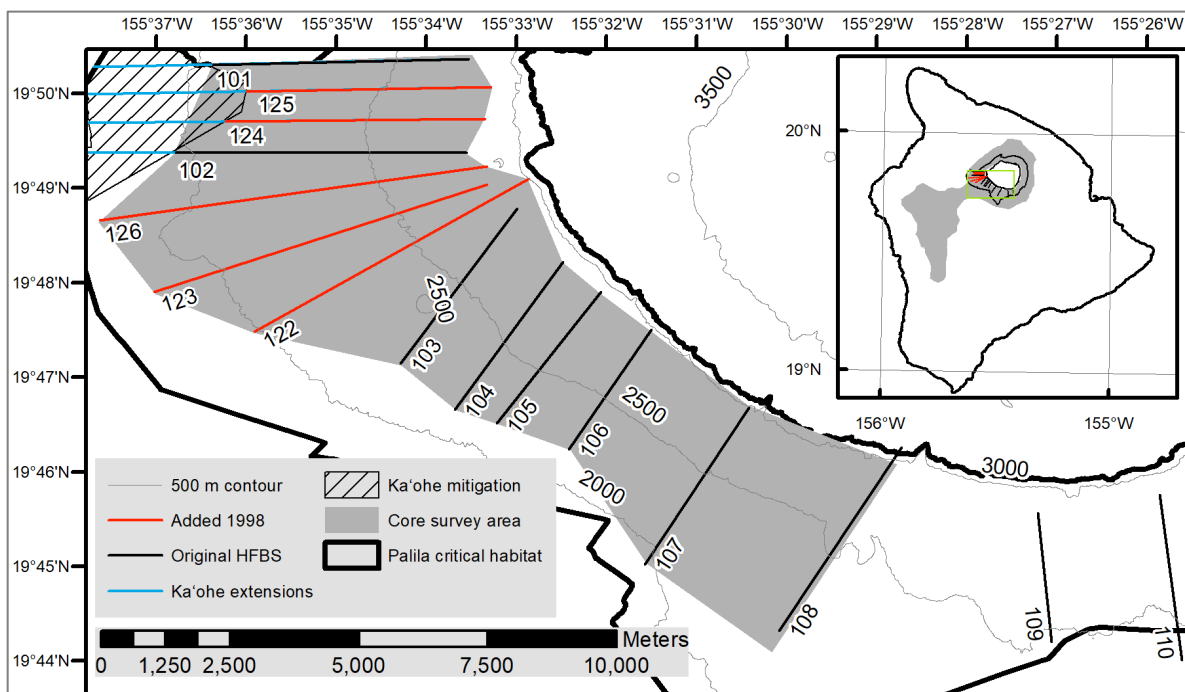


Figure 1. Palila survey area for the 2019–2021 surveys. The area used to estimate palila population abundance is demarcated by the shaded region. Lines depict the original Hawaii Forest Bird Survey (HFBS) transects (black) plus those added in 1998 (red), including supplemental survey effort on transects 109 and 110. Supplemental transect extensions into the Ka’ohe mitigation area are blue. The inset map shows the transects, palila critical habitat (black line), and historical palila range (gray polygon) on Hawai’i Island. Base map from World Geodetic System 1984 (WGS84) zone 5; coastline from U.S. Geological Survey’s National Elevation Dataset (U.S. Geological Survey 2014; contour interval 500 m).

Table 1. Number of transects and stations sampled by year inside and outside the core survey area from 1998 to 2021 on Mauna Kea, Hawai'i Island.

Year	Inside core survey area			Outside core survey area		
	Transects	Stations	Counts	Transects	Stations	Counts
1998	12	355	358	14	186	186
1999	13	417	418	14	192	206
2000	13	418	428	17	224	224
2001	13	416	417	17	223	223
2002	13	417	417	20	270	270
2003	13	404	410	20	258	258
2004	13	399	399	18	244	244
2005	13	403	428	21	352	352
2006	13	386	386	21	353	353
2007	13	408	412	20	253	253
2008	12	387	387	3	53	53
2009	13	416	416	0	0	0
2010	13	415	420	0	0	0
2011	13	411	432	0	0	0
2012	13	420	843	24	426	426
2013	13	418	889	0	0	0
2014	13	407	817	7	115	169
2015	13	420	839	4	63	125
2016	13	420	837	5	79	97
2017	13	420	825	22	367	421
2018	13	419	419	6	97	98
2019	13	417	420	7	83	83
2020	13	419	421	2	23	23
2021	13	420	422	5	74	74

Since the introduction of transects 122–126 in 1998, palila surveys were conducted annually on Mauna Kea, and palila abundance estimates were produced by U.S. Geological Survey (USGS) and partners (Camp and Banko 2012; Camp *et al.* 2014, 2016; Genz *et al.* 2018). Prior to 2008, surveys were conducted mountain-wide, but the lack of detections outside the southwestern slope led to focusing effort on the core survey area with the intent to survey the entire mountain every five years starting in 2012 (David L. Leonard Jr, State of Hawaii, Department of Land and Natural Resources Division of Forestry and Wildlife, oral comm., 2012).

Most forest bird surveys in Hawai'i last eight minutes (Camp *et al.* 2009), however, six minutes is used for palila counts because their woodland habitat is more open than mesic and wet forest habitats, allowing for easier and more rapid detection. Counts commenced at sunrise and continued up to four hours (approximately 11:00 HST). During each count, trained and calibrated observers recorded the species, detection type (heard, seen, or both), and distance of each bird from the observer. Time of sampling and weather conditions (cloud cover, rain intensity, wind strength, and wind gust strength [hereafter gust strength]) were also recorded,

and surveying was postponed when conditions hindered the ability to detect birds (wind and gust strengths >20 kph or heavy rain).

### **Abundance Estimation**

Distance analysis fits a detection function to estimate the probability of detecting a bird at a given distance from the observer where the probability of detection decreases with increasing distance. Previous analysis of palila (Genz *et al.* 2018) showed that the probability of detection was affected not only by distance but also by covariates such as observers, sampling conditions, and survey year. A detection function was fitted to models with and without covariates, accounting for the effect of the observer, detection type, weather conditions, and survey year. Observers with <100 palila detections were combined. Modeling covariates gives better precision, assuming the same model for all factors (Buckland *et al.* 2015). Pooling covariates that have a similarly shaped detection function, based on similar coefficient values, can improve model fit, substantially reduce computation time, and can further increase precision. Detection type was evaluated as heard (detection type = 1) versus seen (detection type = 2) versus first heard then seen (detection type = 4), and where heard was pooled with heard then seen (detection types 1+4 versus 2), and where seen was pooled with heard then seen (detection type 1 versus 2+4). For weather conditions, cloud cover was pooled into counts with no clouds, mostly clear of clouds, and cloudy. Gust strength was pooled into counts with no gust, light gusts, or moderate gusts. Similar to gust strength, wind was pooled into counts with no wind, light winds, or moderate winds. Rain was pooled into counts with and without rain. Years were pooled in five blocks based on similar parameter coefficients (Figure 2). With each additional year of data, estimates of these effects become more precise and the improved detection function may cause population estimates of previous years to change slightly.

Density estimates (birds/km<sup>2</sup>) were calculated from point-transect sampling data using the R (R Core Team 2021) package Distance (version 1.0.3; Miller *et al.* 2019). The 2019–2021 data were pooled with detections from previous surveys since 1998. Candidate models were limited to half-normal and hazard-rate detection functions with expansion series of order two (361, 365; Buckland *et al.* 2001). Survey effort in a given year was adjusted by the number of times the station was counted in that year. To improve model precision, potential sampling covariates were incorporated in the multiple covariate distance sampling engine of Distance. Covariates included the weather conditions, time of sampling, type of detection, observer, and year of survey. The right-tail truncation for the 1998–2018 data was 87.5 m (Genz *et al.* 2018); the distance where the detection probability was 10% in the non-truncated model. The 10% truncation distance in this analysis was 90 m, which is a “heaping” distance (i.e., rounding of distances to favored values). Because Buckland *et al.* (2015) state that a heaping distance should not be selected as a truncation distance, we chose the previous truncation distance of 87.5 m, analogous to truncating approximately 12% of the data. This procedure facilitates modeling by deleting outliers and reducing the number of adjustment parameters needed to modify the detection function. The detection probability model selected was the one having the lowest Akaike’s information criterion (AIC; Buckland *et al.* 2001, Burnham and Anderson 2002). Visual inspection of diagnostic plots was conducted, and model fit was evaluated with a Cramér-von Mises test (Buckland *et al.* 2015). Annual population densities for each survey were calculated using the global detection function, and the pooled data were post-stratified by year and location (inside/outside core survey area). The 95% confidence intervals for the annual density estimates were derived from the 2.5<sup>th</sup> and 97.5<sup>th</sup> percentiles using bootstrap methods in

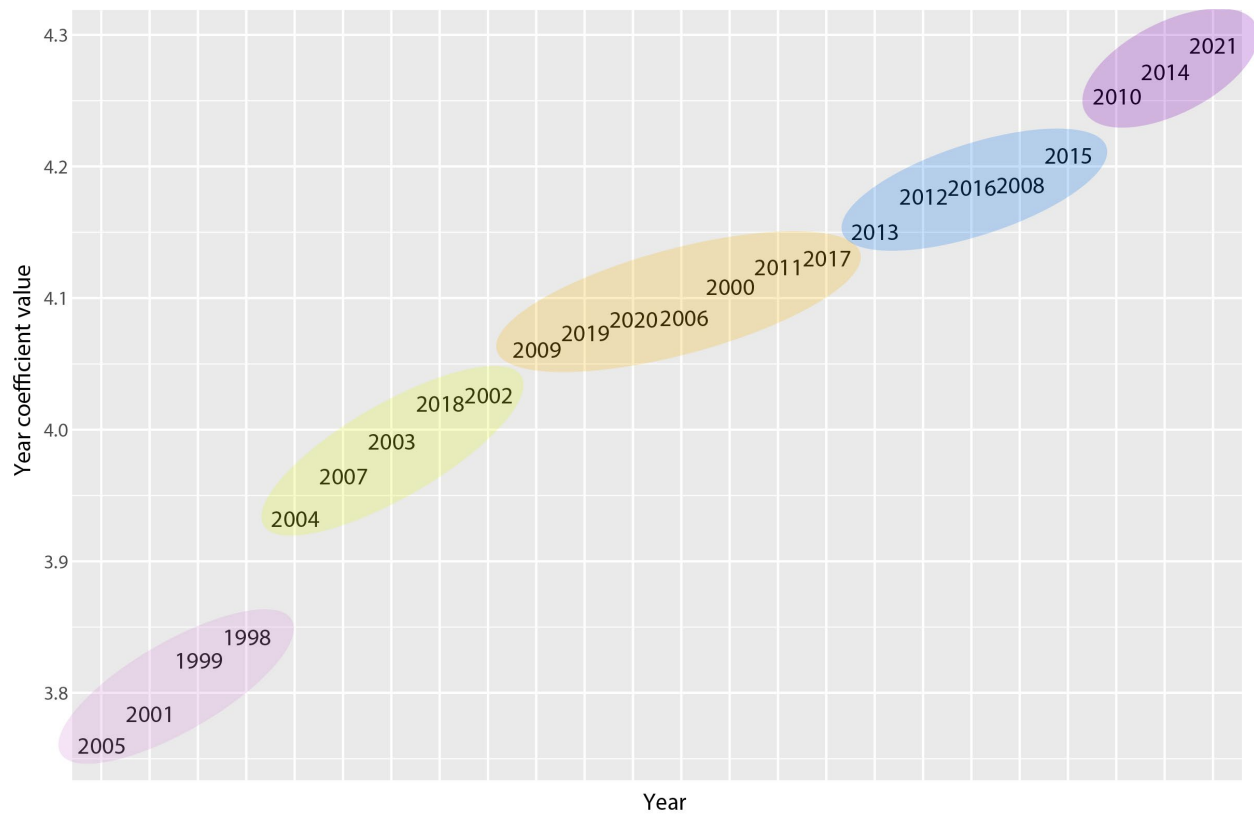


Figure 2. Five blocks of years grouped by the similarity of the parameter coefficients.

Distance for 1,000 iterations (Buckland *et al.* 2001, Thomas *et al.* 2010). Population abundance estimates were the product of the density estimate times the area of the core survey area (64.4 km<sup>2</sup>).

### Trend Detection

The trend in palila abundance was assessed in two different ways. The bootstrap sample estimates generated to evaluate uncertainty in population abundance were used to approximate the long-term population trend (1998–2021) with a log-linear regression model. We evaluated the trend over four time periods—the full modern time span of 23 years, the most recent 15 years, the most recent 10 years, and the most recent 5 years. The evidence of a trend was derived from the bootstrap distribution of slopes, following Camp *et al.* (2015). Diagnostics demonstrated that the log-linear regressions of trends met all model assumptions (visual inspection of residual plots; Shapiro-Wilk normality test,  $w = 0.95$ ,  $P = 0.33$ ), except that some temporal autocorrelation was evident. Because of this, we looked at a lag-one (AR1) autocorrelated model. The best model was the simple log-linear regression with 61% of the AIC weight. The AR1 model had an AIC value <1 unit higher than the base model and the remainder of model weight. In the previous analysis (Genz *et al.* 2018), an AR1 model was used for trend assessment despite having similar AIC weights to the current effort. This was, in part, to be consistent with previous work. However, because the simpler model was preferred by AIC yet again, and because the Bayesian state-space model (see below) provides an inherently auto-correlated alternative trends assessment, we chose to use a simple log-linear model to assess for trend.

We also assessed trend using a Bayesian state-space model on the log-scale. This approach partitions model uncertainty into portions attributable to observation error (due to random noise in the environment affecting detectability and measurement) and process error (due to stochastic fluctuations in population outside of the overall trend). Such a state-space model can be interpreted as a biologically informed smoother and provides annual estimates consistent with the observed inter-annual noise. We used diffuse priors for the model parameters: a normal distribution with mean 0 and standard deviation of 10 for the annual mean population change and exponential priors with mean 0.1 as priors for the standard deviation of slope and the observation error.

The state-space model was fit using the Stan platform (Carpenter *et al.* 2017) run from an R environment using the RStan package (Stan Development Team 2020). The trends were centered on the year 2007 to improve model convergence. The model parameters were estimated from 12,500 iterations for each of four chains (i.e., model runs) after first discarding 500 iterations as a “warm-up” period. The four chains were pooled (50,000 total samples) to calculate the posterior distribution. Gelman-Rubin convergence statistics for all estimated parameters were below 1.01, which is less than the 1.1 threshold that indicates convergence (Gelman and Rubin 1992).

Both methods were assessed in an equivalence-testing approach (Camp *et al.* 2008) using the observed distribution of slopes of the bootstrap distribution and the posterior distribution of the slope from the Bayesian state-space model. We chose biologically meaningful thresholds for the overall population trend as a 25% change in the population over a 25-year period (annual rate of change equal to -0.0119 and 0.0093 [for decreasing and increasing] on the log-scale). A biologically meaningful trend occurs when the posterior probability distribution of the slope lies outside the equivalence region, whereas a negligible trend occurs when the slope is within the equivalence region. An inconclusive result occurs when small sample size and high variation in estimates results in the posterior distribution of the slope providing weak evidence in the three outcomes (increasing, stable, and decreasing). The strength of evidence for a trend was based on the distribution defined as weak, moderate, strong, or very strong based on the percentage of bootstrap slopes in each category: weak if <50%, moderate if between 50% and 70%, strong if between 70% and 90%, and very strong if >90%.

### **Sampling Condition Evaluation**

The sampling conditions, particularly weather that could hinder or prohibit detecting birds, can adversely affect population estimates. We compared the distributions and probability densities of cloud cover, rain, wind, and gust strength by survey year using violin plots. Violin plots are similar to box plots in that they depict the summary statistics of mean, median, and interquartile ranges, but also display the full distribution of the data and include a kernel density to show structures in the data. Assessments were evaluated visually.

## **RESULTS**

### **Abundance Estimation**

Within the 64.4-km<sup>2</sup> core survey area of the southwestern flank of Mauna Kea, the number of palila detected increased by 47% between 2018 and 2019 (99 in 2018 and 146 in 2019). There was a 3% decrease in palila detections between 2019 and 2020 (146 in 2019 and 141 in 2020), and another decrease of 28% between 2020 and 2021 (141 in 2020 and 101 in 2021; Figure 3). The hazard-rate detection function model with year block as the covariate had the lowest AIC

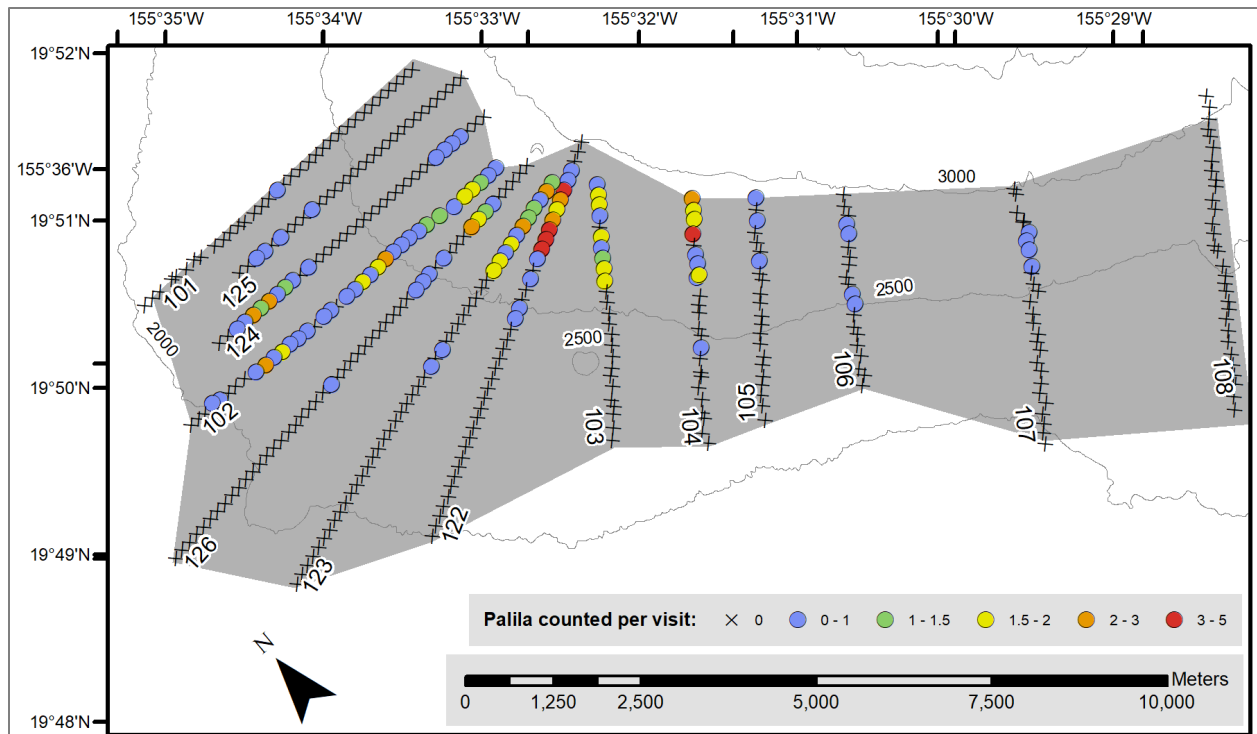


Figure 3. Palila detected per visit across 2019–2021 surveys. X symbols mark stations where no palila were detected during 2019–2021 surveys regardless of survey effort. The shaded region marks the area surveyed to estimate abundance, and transect numbers are included for reference to Figure 1. Graticule tick marks are provided to show geographic coordinates along the border. The map has been rotated to minimize white space. Base map from World Geodetic System 1984 (WGS84) zone 5 (U.S. Geological Survey 2014) (contour interval 500 m).

by >24 units (Table 2, Figure 4). Inspection of diagnostic plots indicated that the model adequately fit the data (Figure 4). The Cramér-von Mises test was non-significant at the  $\alpha = 0.05$  level (test statistic = 0.40,  $P = 0.07$ ) indicating that the detection function did not statistically differ from the distance histogram. An additional four palila were detected in 2019 on the lower extensions of transects 124 and 125 (Table 3). In 2019, the palila population in the core survey area was estimated at 1,030–1,899 birds (point estimate: 1,432; Table 3, Figure 5). In 2020, the palila population in the core survey area was estimated at 964–1,700 birds (point estimate: 1,312). In 2021, the palila population in the core survey area was estimated at 452–940 birds (point estimate of 678).

### Trend Detection

Between 1998 and 2005, palila numbers fluctuated moderately between 4,000 and 6,000 except for a dip in 2000 (Figure 5). After 2005, palila population estimates declined steadily through 2011. During 2010–2021, estimates fluctuated moderately ( $CV = 0.22$ ) with a local peak in 2012. The observed mean decline during 1998–2021 has been 229 birds per year. The bootstrap log-linear regression model showed very strong evidence (posterior probability  $P = 1.0$ ) of a downward trend in palila abundance for all time periods examined. The log-linear

Table 2. Results of fitting 17 detection function models to the 1998–2021 palila distance histogram.  $\Delta$ AIC is the difference in Akaike’s information criterion (AIC) scores between each model and the overall best-fit model, and  $w$  is the discrete model probability. The hazard-rate detection with blocks of years as a factor was chosen (**bold**) as the best model.

Model <sup>1,2</sup>	Number of parameters	AIC	$\Delta$ AIC	$w$
<b>H-rate key yearblock(f)</b>	6	49240.8	0.0	1
H-rate key year(f)	25	49265.0	24.1	0
H-rate key detection type 1 vs 2+4	3	49320.6	79.8	0
H-rate key detection type (1 vs 2 vs 4)	4	49322.3	81.5	0
H-rate key detection type 1+4 vs 2	3	49553.1	312.3	0
H-rate key wind	4	49581.6	340.8	0
H-rate key gust	4	49596.6	355.8	0
H-rate key time	3	49598.1	357.2	0
H-rate key	2	49598.8	358.0	0
H-rate key rain	3	49600.7	359.9	0
H-norm cos(2,3)	3	49601.5	360.7	0
H-rate key cloud	4	49602.8	361.9	0
H-norm herm(4)	2	49621.5	380.6	0
H-norm key	1	49751.3	510.5	0

<sup>1</sup>Models are hazard-rate (H-rate) and half normal (H-norm); adjustment terms are cosine (cos) and Hermite polynomial (herm); and covariates are cloud cover (cloud), detection type (heard, seen, or both; first det. type = pooled heard and both; heard versus seen = pooled visual and both), gust strength (gust), time of detection (time), wind strength (wind), year (year; factor = f), and block year (yearblock; pooled years in 5 blocks; factor = f).

<sup>2</sup>Models H-rate with cosine adjustment term and H-rate with simple polynomial adjustment term indicated the key function as the best model. H-rate key observer model failed to converge. These three models are not included in the table.

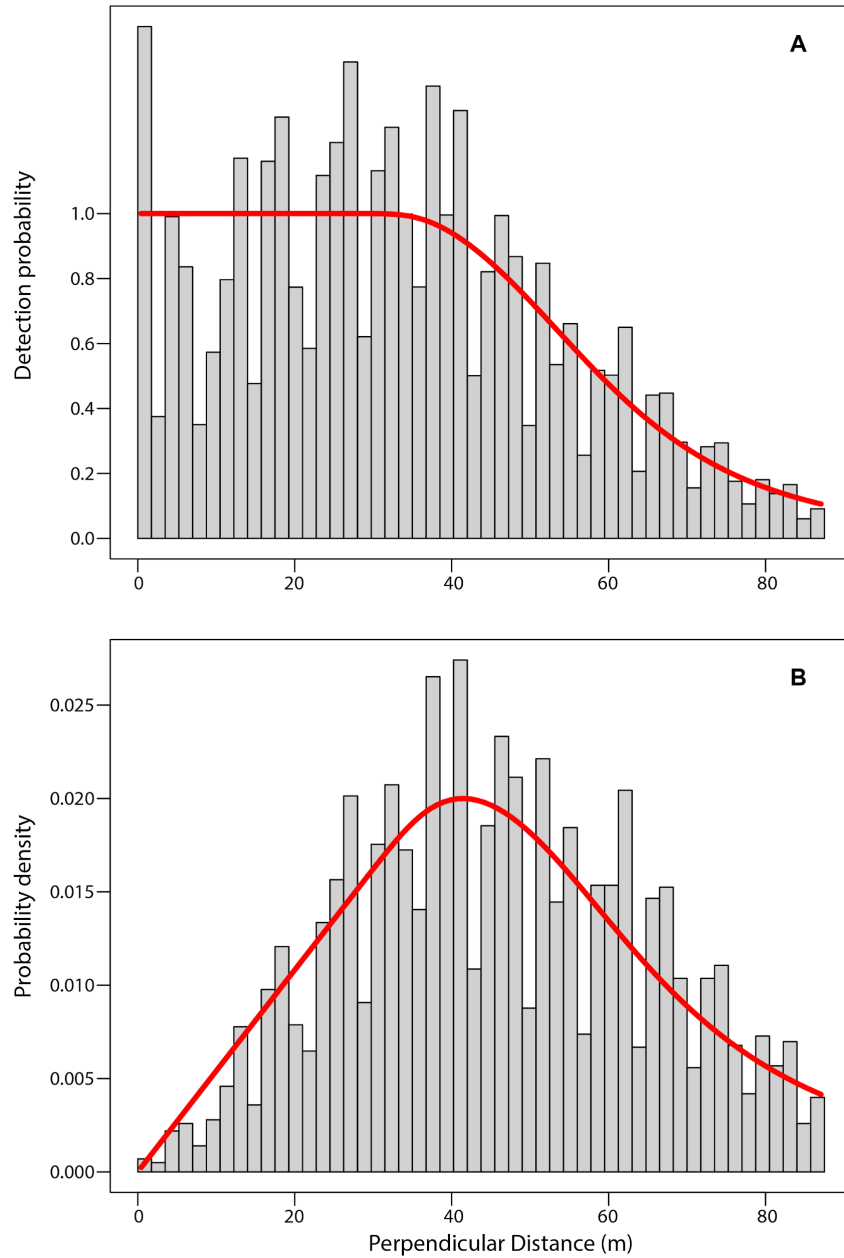


Figure 4. Hazard-rate detection function (A) and probability density (B) of the best-fit detection model. There are no expansion series, and blocked years are included as a detection covariate. The model was fit using palila distance data pooled across all surveys from 1998 to 2021. Data were truncated at 87.5 m. Figure 4B shows how the observed probability distribution of distances (gray bars) matches the modeled detection function, especially at short distances.

Table 3. Annual palila detections and population estimate parameters. Detections are given for palila recorded inside the core survey area and for stations outside the core survey area during six-minute counts. Population parameters include the population estimate, percent coefficient of variation (%CV), standard error (SE), and lower and upper limits of the 95% confidence interval inside the core survey area.

Year	# Detections inside core survey area	# Detections outside core survey area	Estimate	%CV	SE	Lower limit	Upper limit
1998	315	2	5,953	9.8	583	4,894	7,153
1999	389	0	6,840	9.3	634	5,641	8,002
2000	242	12	2,423	10.7	259	1,926	2,937
2001	331	4	5,894	9.8	578	4,795	7,053
2002	339	9	4,294	9.0	385	3,627	5,075
2003	442	4	5,495	9.4	513	4,502	6,567
2004	371	8	4,676	8.8	409	3,934	5,558
2005	315	0	5,448	10.3	560	4,414	6,597
2006	267	15	3,036	10.3	314	2,463	3,673
2007	210	3	2,741	10.6	291	2,182	3,330
2008	192	0	1,842	11.4	210	1,461	2,259
2009	187	na	1,910	12.2	231	1,468	2,379
2010	151	na	981	12.9	125	753	1,231
2011	119	na	1,060	13.8	146	774	1,371
2012 <sup>1</sup>	362	0	1,484	10.7	158	1,189	1,803
2013 <sup>2</sup>	337	na	1,220	9.3	114	1,012	1,458
2014 <sup>3</sup>	351	4	1,244	10.3	128	1,002	1,491
2015 <sup>4</sup>	192	1	774	12.7	98	596	982

2016 <sup>5</sup>	319	4	1,339	11.6	154	1,049	1,653
2017 <sup>6</sup>	248	9	1,192	11.2	134	953	1,472
2018	99	3	1,027	15.9	162	721	1,348
2019	146	4	1,432	15.3	219	1,030	1,899
2020	141	0	1,312	15.0	195	964	1,700
2021	101	0	678	18.7	127	452	940

<sup>1</sup>Of 362 total detections, 194 recorded on first count, 168 recorded on subsequent counts.

<sup>2</sup>Of 337 total detections, 178 recorded on first count, 159 recorded on subsequent counts.

<sup>3</sup>Of 351 total detections, 163 recorded on first count, 188 recorded on subsequent counts.

<sup>4</sup>Of 192 total detections, 99 recorded on first count, 93 recorded on subsequent counts.

<sup>5</sup>Of 319 total detections, 178 recorded on first count, 141 recorded on subsequent counts.

<sup>6</sup>Of 248 total detections, 138 recorded on first count, 110 recorded on subsequent counts.

na = outside core survey area was not surveyed

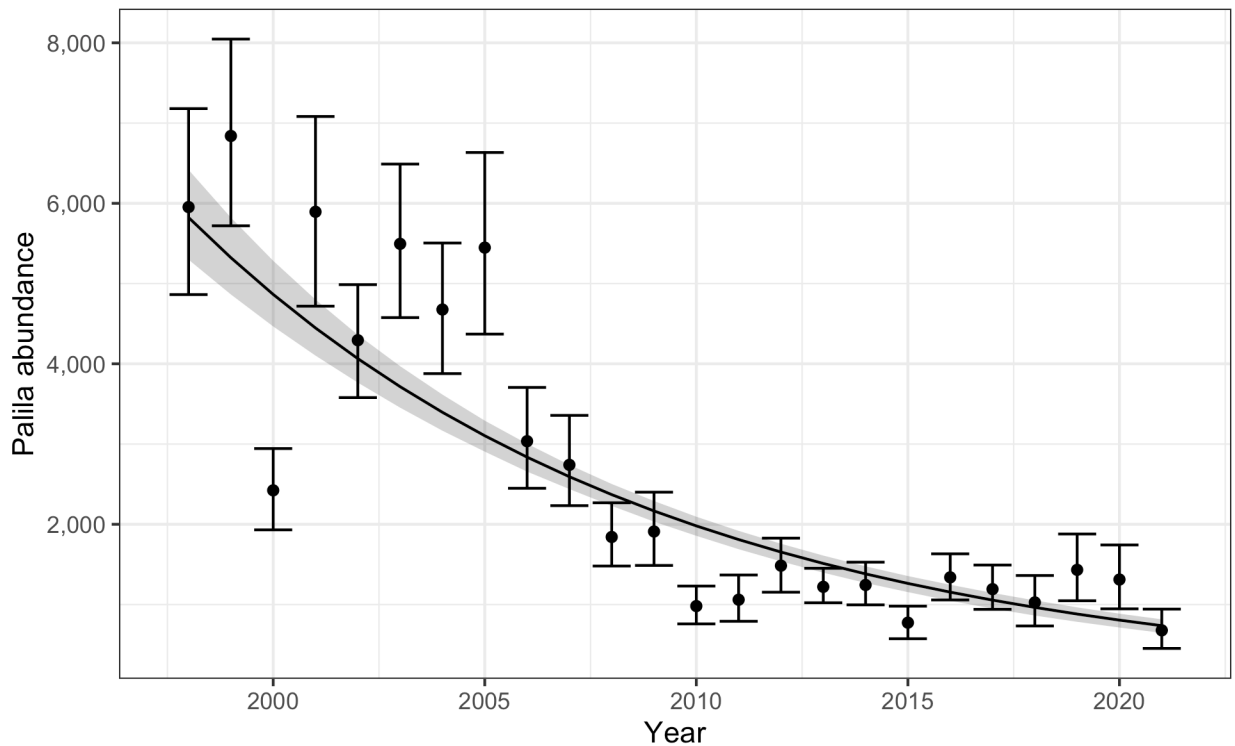


Figure 5. Annual palila population estimates from 1998 through 2021 inside the core survey area on the western slope of Mauna Kea. The line represents the best fit log-linear regression, error bars show 95% bootstrap intervals around the point estimates, and the shaded area shows the 95% band around the bootstrapped regression.

state-space model (Figure 6) also shows very strong evidence of a decline with 79% posterior probability showing a downward trend, only 6% probability of a negligible trend, and 15% for an upward trend. The regression model fit the observed data with a Bayesian  $R^2$  of 0.84, and simulated model runs with log-normal random error were greater than observed errors 56% of the time, where a value of 50% indicates the observed error fit a log-normal distribution exactly (Gelman *et al.* 2004). Figure 6 also shows downward trends for the last 5 years, last 10 years, and last 15 years. Of the three, the trend of the last 10 years is the most optimistic, but still shows only a 31% chance of the population being stable or increasing.

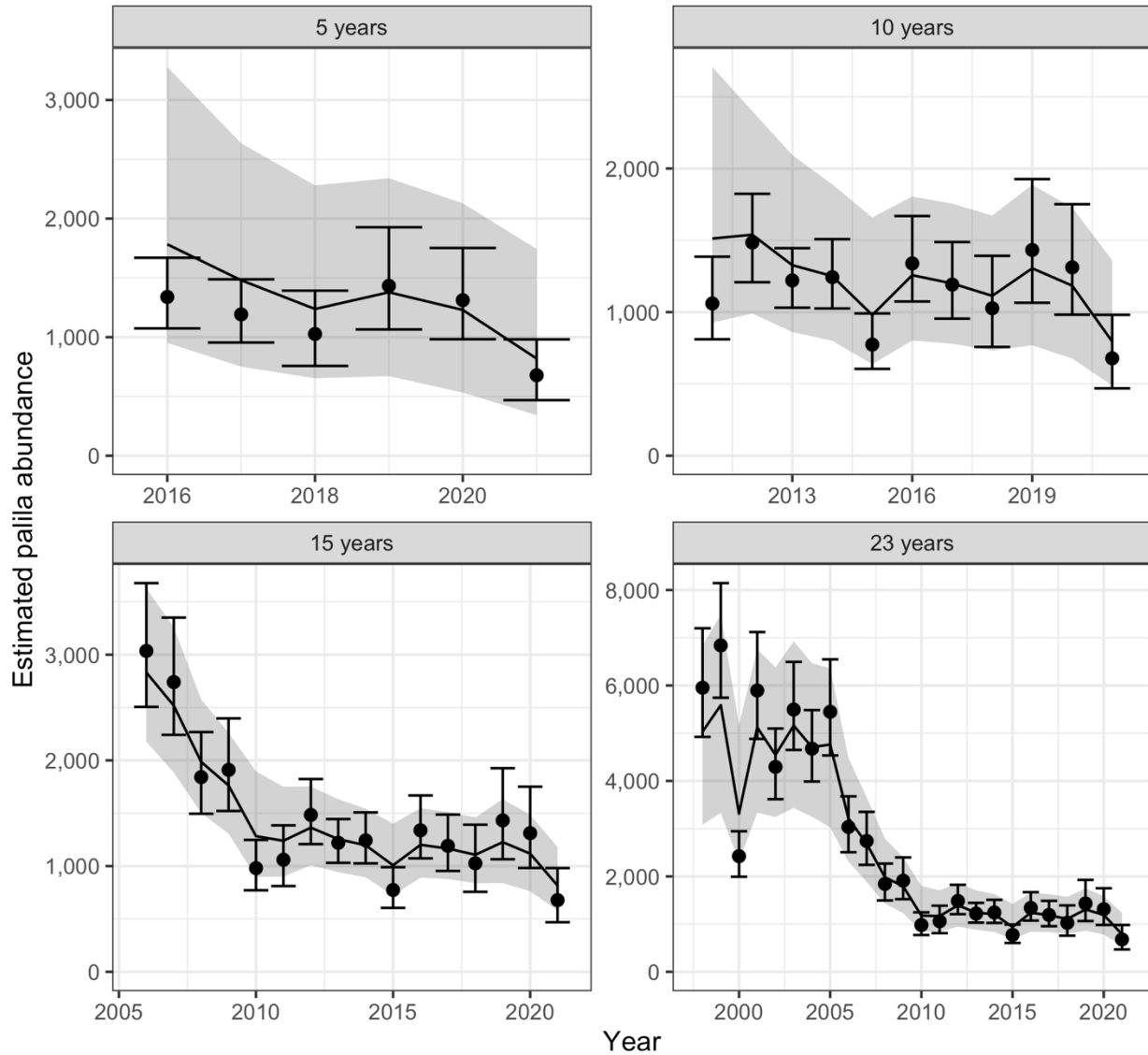


Figure 6. State-space model estimates of palila abundance over multiple time spans—the most recent 5, 10, and 15 years, and the full series from 1998 to 2021 (23-year monitoring period). Points and error bars are estimates from Distance models. The lines show the median estimate from the Bayesian posterior distribution of abundance, and the shaded error shows the 95% credible interval of abundance posteriors.

## Sampling Condition Evaluation

The 2021 abundance estimates are about half that of 2020 estimates, which is biologically unlikely. Similar to 2021, abundance estimates declined more than 35% in 2000, 2010, and 2015, immediately after which estimates increased. Weather conditions during these surveys did not contribute to low estimates as they did not differ markedly from conditions during other surveys (Figure 7). This is because surveys were halted when sampling conditions hindered detecting birds (e.g., heavy rains or strong winds).

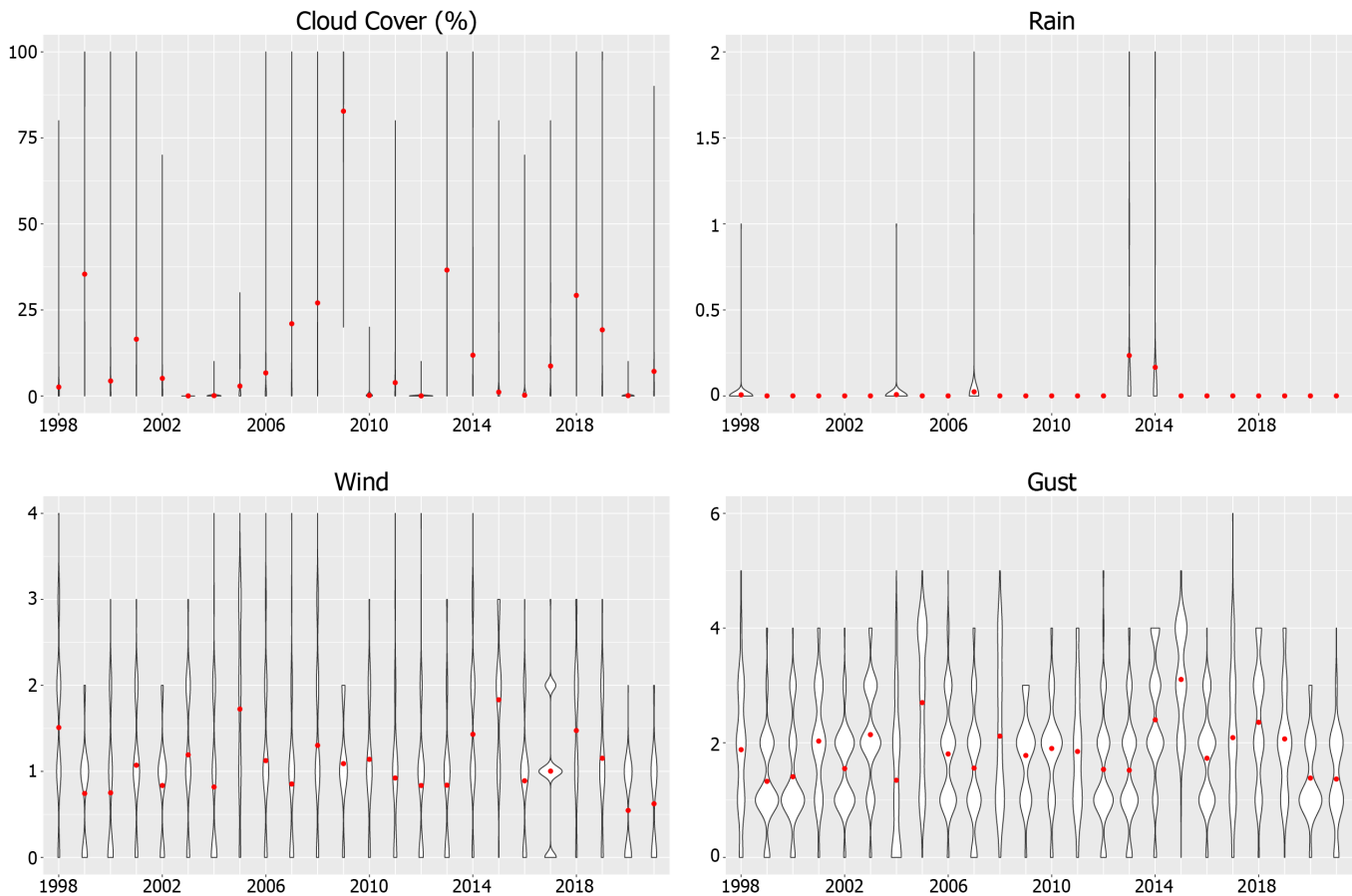


Figure 7. Violin plots of weather covariates for each survey year. Red dots depict the mean value at each year. Cloud cover was recorded at the nearest 10%. Rain values were recorded as categories between zero and four, with zero equaling no rain and four equaling heavy rain. Wind speed was recorded on the Beaufort scale from zero to five, with zero equaling calm conditions and five equaling strong breeze. Gust is the maximum wind speed and was recorded on the Beaufort scale.

## CONCLUSIONS

The 2021 palila population was estimated at 452–940 birds (point estimate of 678) or roughly half the number estimated in the two preceding years—the 2019 estimated population was 1,030–1,899 birds (point estimate of 1,432), and the 2020 estimated population was 964–1,700 birds (point estimate of 1,312). There was very strong evidence that the palila

population has declined since the current survey transects were implemented in 1998. Table 3 and Figure 5 show the population fluctuating in the 4,000–6,000 range (except in 2000) from 1998 to 2005, at which point a steep decline began. Beginning around 2010 the steep decline appears to level off (around an abundance of 2,000), but the trend assessments show that population continues to decline, leading to a record low in 2021.

The mean decline during 1998–2021 was 229 birds per year, resulting in an 89% decline in the population over the 23-year monitoring period. In this report we produced trend assessments for a range of time spans to examine how different time periods might affect conclusions. In strict practice the time frame for a trend assessment is best determined before the data are analyzed to avoid post-facto choices to arrive at a desired conclusion, so for our purposes the trend across the full 23-year span is definitive. Figure 5 shows that different trends (possibly due to different population dynamics or environmental effects) are operating in the 1998–2021 time span. Future analyses may wish to specify an assessment beginning after the decline seems to have leveled off, or for the previous 10 years, to measure the effect of current population and environmental conditions.

The palila population is almost certainly continuing to decline. The most optimistic method (state-space assessment for the most recent 10 years) shows only a 31% chance of the trend being stable or upward. Based on the methods used and estimates reported in Johnson *et al.* (2006), the estimated abundance of palila in 2021 is the lowest since regular surveys began in 1980. The weather conditions in 2021 were not markedly different from those of previous surveys, nor were the conditions different during other years when estimates were low (e.g., 2000, 2010, and 2015), thus are not likely to contribute to the low estimates. In the 2017 mountain-wide survey, no palila were detected along the southeastern and eastern slopes of Mauna Kea, where they have been detected historically, but there were two detections on the north slope, where wild birds were translocated (1997–1998, 2004–2006), and captive-reared birds were released (2003–2005, 2009 [Banko and Farmer 2014], and 2019 [Matsuoka *et al.* 2021]). There were also palila detected outside the core survey area at lower elevation, indicating that they may be using former pasture lands that have been removed from grazing and subject to reforestation implemented through the Mauna Kea Forest Restoration Project ([dlnr.hawaii.gov/restoremaunakea/](http://dlnr.hawaii.gov/restoremaunakea/)). Still, the palila range is only about 5% of its historical extent (Figure 1 inset; Banko *et al.* 2013).

## ACKNOWLEDGEMENTS

Support for the annual palila surveys since 1998 was provided by the Federal Highway Administration, U.S. Army Garrison Hawaii, Hawaii Department of Land and Natural Resources (DLNR) Division of Forestry and Wildlife, U.S. Fish and Wildlife Service State Wildlife Grant Program, American Bird Conservancy, National Fish and Wildlife Foundation, and the U.S. Geological Survey Wildlife Program. Funding for analyses of the data since 2012 was provided by the Hawaii DLNR Division of Forestry and Wildlife. We are grateful to the many agency staff and volunteers who helped collect survey data and to Chris Farmer and Chris Warren for reviews of an early draft. Editorial and online publishing support provided by Sarah Nash through the Hawai'i Cooperative Studies Unit. Data and metadata associated with this report from 1998 to 2018 are available at <https://doi.org/10.5066/P9DO0PL4> (Brinck *et al.* 2018), and data from 2019 to 2021 are available from the DLNR upon request.

## LITERATURE CITED

- Banko, P. C., and C. Farmer (editors). 2014. Palila restoration research, 1996–2012. Hawai'i Cooperative Studies Unit Technical Report HCSU-046. University of Hawai'i at Hilo, Hawaii, USA. 499 pp.
- Banko, P. C., K. W. Brinck, C. Farmer, and S. C. Hess. 2009. Recovery programs: palila. Chapter 23, pp. 513–529 in T. K. Pratt, C. T. Atkinson, P. C. Banko, J. D. Jacobi, and B. L. Woodworth (editors). Conservation Biology of Hawaiian Forest Birds: Implications for Island Avifauna. Yale University Press, New Haven, Connecticut, USA.
- Banko, P. C., L. Johnson, G. D. Lindsey, S. G. Fancy, T. K. Pratt, J. D. Jacobi, and W. E. Banko. 2002a. Palila (*Loxioides bailleui*). No. 679 in A. Poole and F. Gill (editors). The Birds of North America. The Birds of North America, Inc., Philadelphia, Pennsylvania, USA.
- Banko, P. C., P. T. Oboyski, J. W. Slotterback, S. J. Dougill, D. M. Goltz, L. Johnson, M. E. Laut, and C. Murray. 2002b. Availability of food resources, distribution of invasive species, and conservation of a Hawaiian bird along a gradient of elevation. *Journal of Biogeography* 29:789–808.
- Banko, P. C., R. J. Camp, C. Farmer, K. W. Brinck, D. L. Leonard, and R. M. Stephens. 2013. Response of Palila and other subalpine Hawaiian forest bird species to prolonged drought and habitat degradation by feral ungulates. *Biological Conservation* 157:70–77.
- Brinck, K. W., A. S. Genz, and R. J. Camp. 2018. Mauna Kea Palila point count data from annual surveys 1998–2018 (Ver. 2.0, January 2022). U.S. Geological Survey data release, <https://doi.org/10.5066/P9DO0PL4>.
- Buckland, S. T., D. R. Anderson, K. P. Burnham, J. L. Laake, D. L. Borchers, and L. Thomas. 2001. Introduction to Distance Sampling: Estimating Abundance of Biological Populations. Oxford University Press, Oxford, UK. 448 pp.
- Buckland, S. T., E. A. Rexstad, T. A. Marques, and C. S. Oedekoven. 2015. Distance Sampling: Methods and Applications. Springer International Publishing, Cham, Switzerland. 277 pp.
- Burnham, K. P., and D. R. Anderson. 2002. Model selection and multimodel inference: a practical information-theoretic approach. Second edition. Springer-Verlag, New York, New York, USA.
- Camp, R. J., K. W. Brinck, and P. C. Banko. 2014. Palila abundance estimates and trend. Hawai'i Cooperative Studies Unit Technical Report HCSU-053. University of Hawai'i at Hilo, Hawaii, USA. <http://hdl.handle.net/10790/2611>
- Camp, R. J., K. W. Brinck, and P. C. Banko. 2016. 2015–2016 Palila abundance estimates. Hawai'i Cooperative Studies Unit Technical Report HCSU-076. University of Hawai'i at Hilo, Hawaii, USA. <http://hdl.handle.net/10790/2750>
- Camp, R. J., K. W. Brinck, P. M. Gorresen, F. A. Amidon, P. M. Radley, S. P. Berkowitz, and P. C. Banko. 2015. Current land bird distribution and trends in population abundance between 1982 and 2012 on Rota, Mariana Islands. *Journal of Fish and Wildlife Management* 6(2). <https://doi.org/10.3996/112014-JFWM-085>
- Camp, R. J., M. Gorresen, T. K. Pratt, and B. L. Woodworth. 2009. Population trends of native Hawaiian forest birds: 1976–2008. Hawai'i Cooperative Studies Unit Technical Report HCSU-012. University of Hawai'i at Hilo, Hawaii, USA. <http://hdl.handle.net/10790/2692>

- Camp, R. J., N. E. Seavy, P. M. Gorresen, and M. H. Reynolds. 2008. A statistical test to show negligible trend: comment. *Ecology* 89:1469–1472.
- Camp, R. J., and P. C. Banko. 2012. Palila abundance estimates and trend. Hawai'i Cooperative Studies Unit Technical Report HCSU-033. University of Hawai'i at Hilo, Hawaii, USA. <http://hdl.handle.net/10790/2630>
- Carpenter, B., A. Gelman, M. D. Hoffman, D. Lee, B. Goodrich, M. Betancourt, M. Brubaker, J. Guo, P. Li, and A. Riddell. 2017. Stan: A probabilistic programming language. *Journal of Statistical Software* 76:1–32. <https://doi.org/10.18637/jss.v076.i01>
- Gelman, A., and D. B. Rubin. 1992. Inference from iterative simulation using multiple sequences. *Statistical Science* 7:457–511.
- Gelman, A., J. B. Carlin, H. S. Stern, and D. B. Rubin. 2004. Bayesian data analysis, second edition. Chapman & Hall, New York, New York, USA.
- Genz, A. S., K. W. Brinck, R. J. Camp, and P. C. Banko. 2018. 2017–2018 Palila abundance estimates and trend. Hawai'i Cooperative Studies Unit Technical Report HCSU-086. University of Hawai'i at Hilo, Hawaii, USA. <http://hdl.handle.net/10790/4431>
- Gorresen, P. M., R. J. Camp, M. H. Reynolds, T. K. Pratt, and B. L. Woodworth. 2009. Status and trends of native Hawaiian songbirds. Chapter 5, pp. 108–136 *in* T. K. Pratt, C. T. Atkinson, P. C. Banko, J. D. Jacobi, B. L. Woodworth (editors). *Conservation Biology of Hawaiian Forest Birds: Implications for Island Avifauna*. Yale University Press, New Haven, Connecticut, USA.
- Hess, S. C., P. C. Banko, M. H. Reynolds, G. J. Brenner, and L. P. Laniawe. 2001. Seasonal changes in food resource abundance and drepanidine densities in subalpine woodland on Mauna Kea, Hawai'i. *Studies in Avian Biology* 22:154–163.
- Jacobi, J. D., S. G. Fancy, J. G. Giffin, and J. M. Scott. 1996. Long-term population variability in the palila, an endangered Hawaiian honeycreeper. *Pacific Science* 50:363–370.
- Johnson, L., R. J. Camp, K. W. Brinck, and P. C. Banko. 2006. Long-term population monitoring: lessons learned from an endangered passerine in Hawai'i. *Wildlife Society Bulletin* 34:1055–1063.
- Leonard, Jr., D. L., P. C. Banko, K. W. Brinck, C. Farmer, and R. J. Camp. 2008. Recent surveys indicate rapid decline of palila population. *'Elepaio* 68:27–30.
- Matsuoka, K., J. Tupu, A. Lilly, A. Bischer, L. Berry, J. Gaudioso-Levita, A. Wang, K. Asing, K. Brinck, and B. Masuda. 2021. Palila release 2019 summary. Unpublished report to the Palila Hui, a joint working group of the U.S. Fish and Wildlife Service, American Bird Conservancy, Hawaii Department of Land and Natural Resources-Division of Forestry and Wildlife, San Diego Zoo Wildlife Alliance, University of Hawai'i-Pacific Cooperative Studies Unit, and U.S. Geological Survey.
- Miller, D. L., E. Rexstad, L. Thomas, L. Marshall, and J. L. Laake. 2019. Distance sampling in R. *Journal of Statistical Software* 89(1):1–28. <https://doi.org/10.18637/jss.v089.i01>
- R Core Team. 2021. R: A language and environment for statistical computing. R Foundation for Statistical Computing, Vienna, Austria. <http://www.R-project.org/>.

- Scott, J. M., S. Mountainspring, C. van Riper III, C. B. Kepler, J. D. Jacobi, T. A. Burr, and J. G. Giffin. 1984. Annual variation in the distribution, abundance, and habitat response of the palila (*Loxioides bailleui*). *Auk* 101:647–664.
- Stan Development Team. 2020. RStan: the R interface to Stan. R package version 2.21.2. <http://mc-stan.org/>.
- Thomas, L., S. T. Buckland, E. A. Rextad, J. L. Laake, S. Strindberg, S. L. Hedley, J. R. B. Bishop, T. A. Marques, and K. P. Burnham. 2010. Distance software: design and analysis of distance sampling surveys for estimating population size. *Journal of Applied Ecology* 47:5–14.
- USGS (U.S. Geological Survey). 2014. National elevation dataset (NED): U.S. Geological Survey database. <<http://national-map.gov/elevation.html>>, accessed 25 Sep 2014.